F.K. Knight, S.R. Kulkarni, R.M. Marino, and J.K. Parker

Tomographic Techniques Applied to Laser Radar Reflective Measurements

Methods of tomography are applied to laser radar reflective measurements to study remote imaging of macroscopic objects. Techniques to produce 2-D images from 1-D data and 3-D images from 2-D data are described, and examples are shown. The data are the received signals from laser radars, resolved in either 1-D (range or Doppler) or 2-D (angle-angle) and taken from many viewing directions. Examples are presented of reconstructed images of laboratory test objects obtained with infrared and visible laser radars. Each reconstructed image depicts the object's geometric features. Prospects for future applications are discussed.

This article describes the application of tomographic image-reconstruction techniques to measurements made with laser radar remote sensors. Tomographic methods are used to reconstruct an image from a set of its projections and have been applied to many fields, e.g., radio astronomy and medical imaging [1, 2]. Here we use a well-developed technique of tomography to combine laser radar reflective measurements taken from many viewing directions. The result is an image of the illuminated object. We discuss the reconstruction of 2-D images from 1-D data and the reconstruction of 3-D images from 2-D data. This article reviews work reported in more detail elsewhere [3–5].

As in X-ray absorption CAT scans, the goal of 2-D transmission tomography is to estimate the spatial dependence of the absorption of a penetrating radiation—based on a series of 1-D projections of a slice of an object. Transmission tomography utilizes a line of detectors to resolve the absorption characteristics of the object along an axis perpendicular to the line of sight (LOS) of the detector. The signal from each detector is the integrated absorption along the LOS through the object, so that a line of detectors produces a 1-D absorption projection of the object. The absorption at each point in the slice can be estimated from a series of such projections measured in angular increments around the object.

In the laser radar measurements discussed here, the object is resolved in either range, Doppler (velocity), or angle. The signal in each resolution cell represents the energy reflected off the corresponding illuminated surface of the object. A series of signals along the resolution coordinate produces a reflective projection of the object. The goal of reflective tomography is to estimate object surface features based on a set of reflective projections that are measured in angular increments around the object.

While the two types of measurements—transmission and reflective—are fundamentally different, as shown in Fig. 1, there are similarities in the collected data. The sensor geometries associated with looking around the respective objects can be similar. Also, radar reflective measurements can be interpreted as weighted projections of the object's radar cross section along the direction in which the object is resolved. For these reasons, techniques of transmission tomography can be applied to reflective measurements to yield information about the surface features of the object [3–13]. (See the box, "Transmission and Reflective Tomography," for an illustration of reflective and transmission tomography.)

This article describes three types of radar data (range-resolved, Doppler-resolved, and angle-angle-resolved) and a standard method of image reconstruction from projections (filtered back-projection). Laboratory and field measurements that use the three radar types are pre-

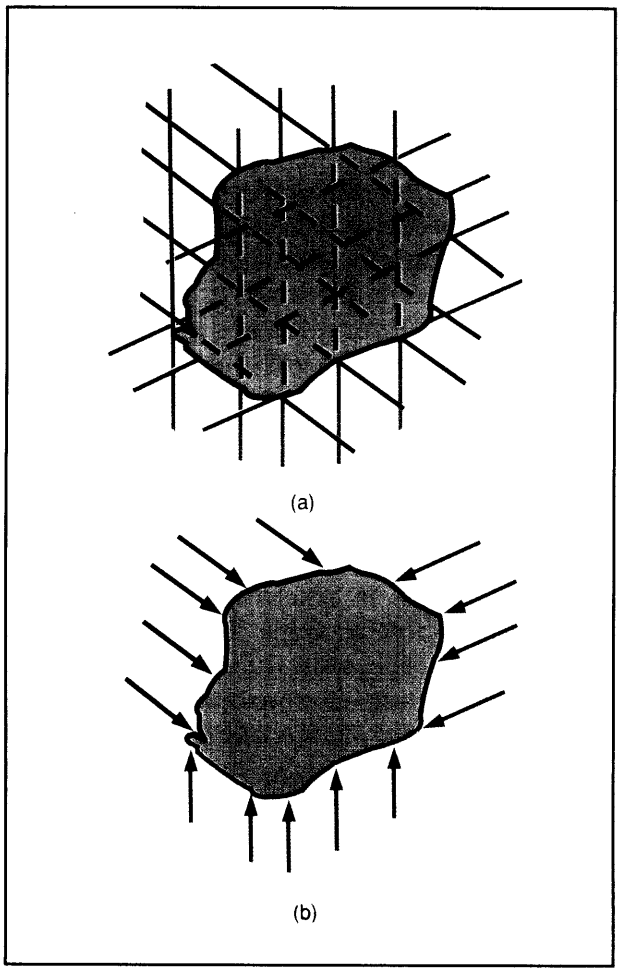

Fig 1—A diagram of two types of tomography distribution. (a) In transmission tomography, transmission through the object is used to reconstruct the interior mass. (b) In reflective tomography, light reflected off the surface of the object is used to reconstruct surface features.

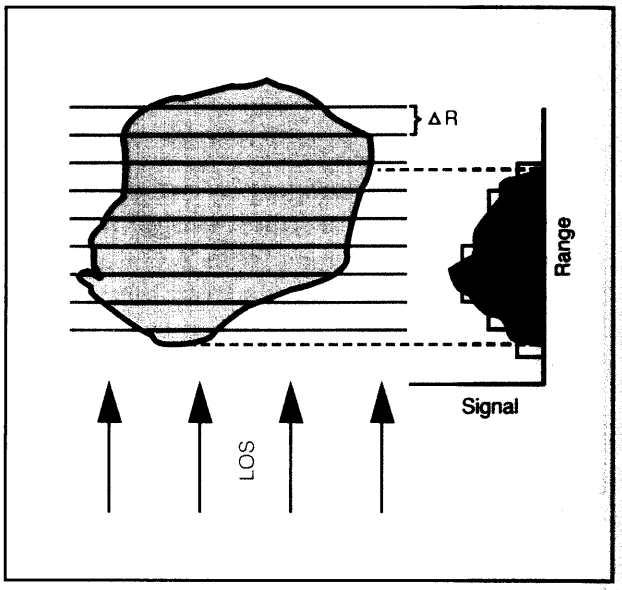

Fig. 2—A range-resolving radar views an object whose depth is greater than the range resolution ΔR. The receiver detects a signal (blue), which is a continuous function of range, and produces a histogram (red) with a cell size ΔR. The magnitude of the received signal depends on the surface area and orientation in each cell, and on the material reflectance.

sented. Doppler-resolved projections of an object are measured with a narrowband infrared laser radar; range-resolved and angle-angle-resolved reflective projections are measured with a short-pulse visible laser radar. These measurements serve as examples of data sets taken from many viewing directions and are used as input to the tomographic reconstruction algorithms.

Laser Radar Measurements

Laser radars can be designed to provide a variety of data from remote objects. With sufficient angular resolution, an object can be imaged in angle to yield a 2-D angle-angle signature. With sufficient range resolution, the object's reflective signature can be resolved in a 1-D range dimension. Similarly, with relative rotation between the object and the sensor, and sufficient Doppler resolution, the object's reflective signature can be resolved in a 1-D Doppler dimension. For any laser radar, the received signal represents information about the *surface* of the object illuminated by the radar from a given LOS.

Consider an object illuminated by a range-resolving radar, either with short pulses or with frequency modulation, as shown in Fig. 2. The received signal is separated into time or frequency cells, each corresponding to a range extent ΔR. We are interested in the case in which ΔR is less than the projected depth of the

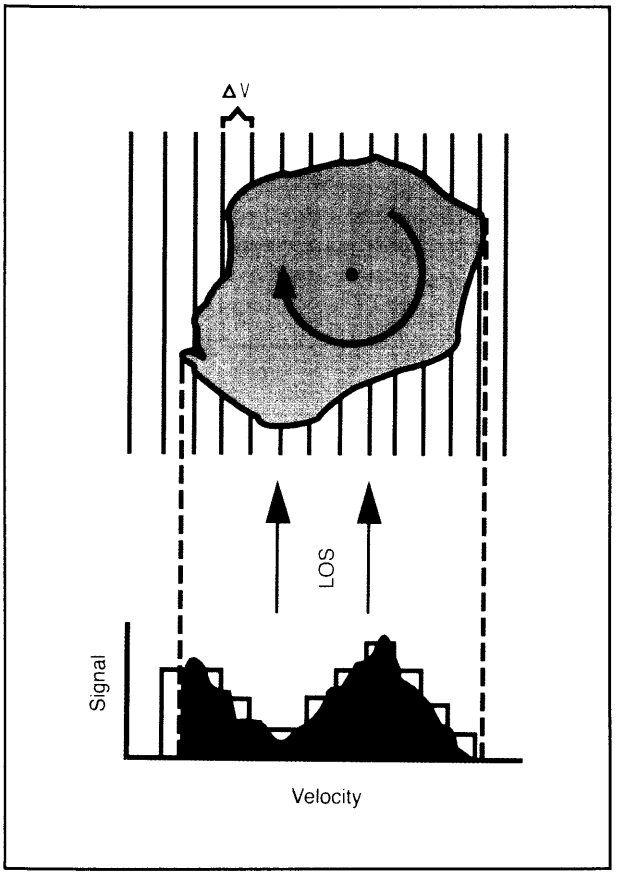

Fig. 3—A Doppler-resolving radar views a rotating object whose velocity spread is greater than the velocity resolution ΔV. *The receiver detects a signal (blue), which is a continuous function of velocity, and produces a histogram (red) with a cell size* ΔV. *The magnitude of the received signal depends on the surface area and orientation in each velocity cell and on the material reflectance.*

object, so that the object is resolved in range. Each cell that receives a signal from the object contains reflected radiation from all unshadowed portions of the object's surface in a slice of range extent ΔR. For a radar pulse of duration τ or a bandwidth $B = 1/\tau$,

$$\Delta R = \frac{c\tau}{2} = \frac{c}{2B}$$

where c is the speed of light. The visible radar used for range-resolved measurements has τ = 250 ps, which yields a range resolution of about 4 cm. This resolution is sufficient to show details on meter-sized objects.

Alternatively, consider an object illuminated by a Doppler-resolving radar, as shown in Fig. 3. The frequency of the received signal is shifted by an amount proportional to the object's velocity component along the radar LOS. If the object is spinning, the received signal is spread in frequency because of the variation of the LOS component of velocity across the object's surface. The received signal is separated into frequency cells; each cell corresponds to an interval of projected velocity ΔV. We are interested in the case in which ΔV is less than the projected velocity spread of the object, so that the object is resolved in velocity. The Doppler-resolved measurement for a spinning object represents a cross-range projection of the object weighted by the reflectance of the surface. Velocity resolution ΔV can be achieved with a narrowband waveform of carrier frequency ν and duration τ, where

$$\Delta V = \frac{c}{2\nu\tau} .$$

The infrared Doppler radar used for the Doppler-resolved measurements is a continuous-wave radar sampled with a time window τ of 1 ms. The wavelength of 10.6 μm or a frequency of ν = 28 THz yields a velocity resolution of 0.52 cm/s. For a 1-m diameter cone, spinning at 1 rpm, oriented perpendicular to the LOS, the spread of projected velocity is ±5.2 cm/s, which yields 20 cells across the cone.

Two-dimensional images can be obtained directly with a laser radar that resolves the object in angle-angle dimensions, as shown in Fig. 4. In an angle-angle measurement, the object is resolved in angular pixels across the object field. The resolution of angle-angle imaging is determined by the diameter D of the optics, the wavelength λ, and the size of the detector elements. For diffraction-limited performance, the resolution is proportional to λ/D. The visible radar used for the angle-angle measurements has a TV camera with 300 × 300 angular pixels over a field of view of 17° diameter. The pixels on

Transmission and Reflective Tomography

A simple example illustrates the functional similarities between transmission tomography and reflective tomography. Figure A shows an empty rectangular box of uniform wall mass density and thickness. Three separate transmission projections $p(u, \phi)$ of the empty box, taken from viewing directions ϕ_1, ϕ_2, and ϕ_3 (= ϕ_2 + 180°), are shown. The two peaks of each projection are due to the increased absorption from the two walls that have normals perpendicular to the LOS for each measurement. Notice that the projections of ϕ_2 and ϕ_3 contain the same information. In general, measurements made from 180° to 359° contain no more information than those made from 0° to 179°.

Figure B shows range-resolved reflective projections $p(u, \phi)$ measured from the same object with a laser radar. To the laser radar the walls of the object are opaque, and the strong reflection from the face nearest the sensor, which is normal to the LOS for viewing directions ϕ_1, ϕ_2, and ϕ_3 (= ϕ_2 + 180°), dominates each projection. Unlike the transmission case, the projections of ϕ_2 and ϕ_3 do not measure the same features (in this case, the same surfaces). Thus, measurements over a full 360° are required for nonsymmetric or unknown objects. Notice the similar shape of the range-resolved projection $p(u_2, \phi_2) + p(u_3, \phi_3)$ with those of the transmission projections. The similarity leads to an interesting observation. A series of transmission projections taken from a *hollow* object can reconstruct the outline of the object, whereas a series of range-resolved reflective projections can reconstruct an image resembling the projected outline of an *opaque* object.

Figure C illustrates an opaque box with Doppler-resolved reflective projections taken from the same three directions. Again colinear measurements taken from opposite directions do not contain the same information. Although the Doppler-resolved projections don't resemble the transmission projections, tomographic techniques can still be applied to yield reconstructions that show object features but not necessarily outlines.

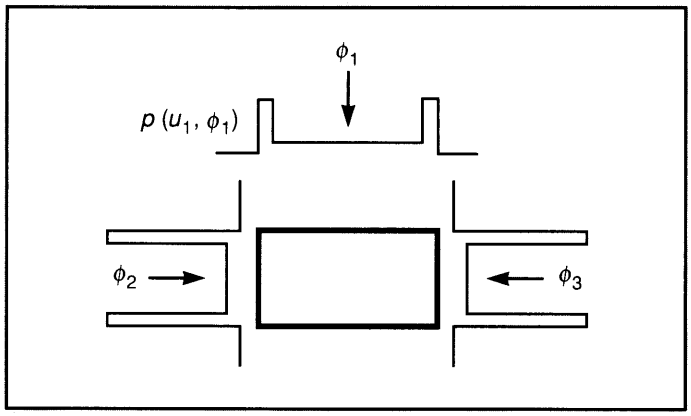

Fig. A—Three transmission projections of a hollow box. Notice that the projections from ϕ_2 and from ϕ_3 (= ϕ_2 + 180°) contain the same information.

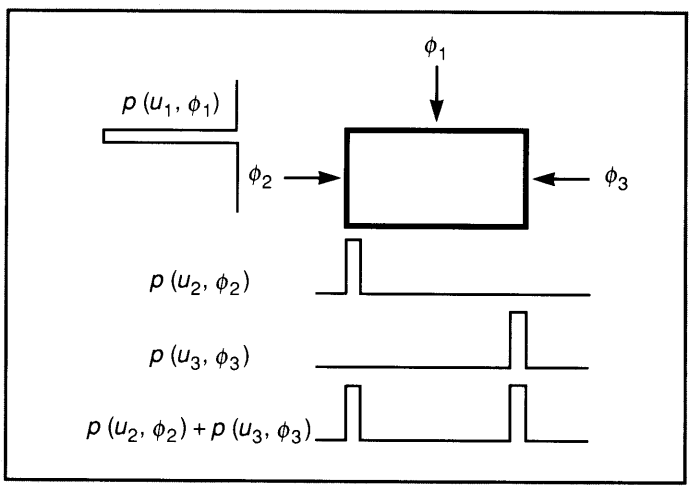

Fig. B—Three range-resolved reflective projections of a hollow diffuse box. Notice that the combined projection p(u, ϕ) + p(–u, ϕ + 180°) has a shape similar to the transmissive projections of Fig. A.

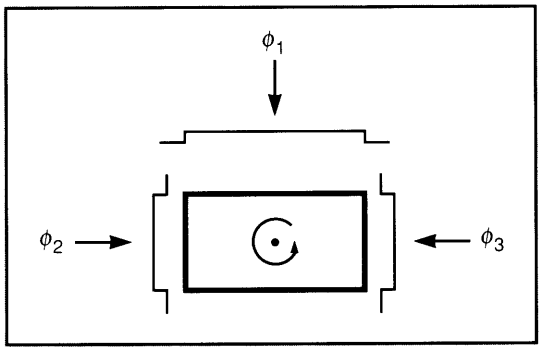

Fig. C—Three Doppler-resolved reflective projections of a rotating hollow diffuse box. Notice that these projections do not clearly resolve the faces of the box.

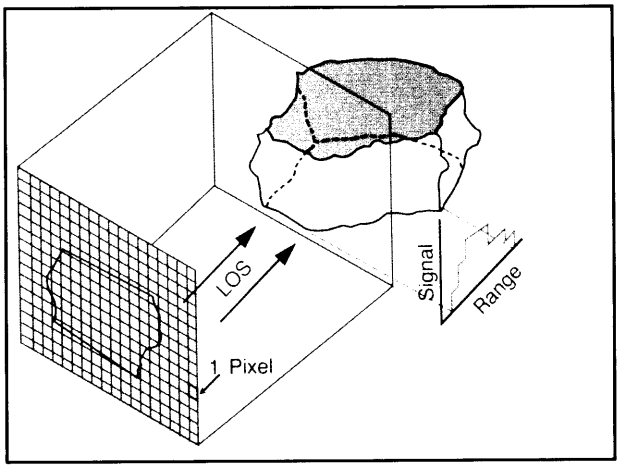

Fig. 4—An angle-angle radar illuminates the object of Figs. 2 and 3 from the same line of sight. The perspective view is from the side and not the top as in Figs. 2 and 3. The angle-angle signal is a digital photograph of the object; pixel boundaries are shown in red. For comparison, the signal (green) from the range-resolving radar of Fig. 2 is shown in perspective.

an object at a range of 10 m are 1 cm × 1 cm. These dimensions, although not diffraction-limited, are sufficient to show details on meter-sized objects.

Reconstruction Method

A number of methods for transmission tomography have been developed and described in Refs. 1 and 2. We have considered and compared some of the methods as applied to laser radar data [5]. This section describes one standard tomographic method known as filtered back-projection.

First, notation and definitions are required. Let $g(x, y)$ denote the image to be reconstructed, and let $L_{u,\phi}$ denote the line $u = x\cos\phi + y\sin\phi$. Let $p(u, \phi)$ denote the integral of $g(x, y)$ along $L_{u,\phi}$, i.e.,

$$p(u, \phi) = \int_{L_{u,\phi}} g(x, y)\, ds$$

where s represents arc length along $L_{u,\phi}$ (Fig. 5). For a fixed ϕ, $p(u, \phi)$ as a function of u is called the projection of $g(x, y)$ in the direction ϕ.

The simplest algorithm for image reconstruction estimates the image $g(x, y)$ by spreading (back-projecting) the values of individual projections $p(x\cos\phi_i + y\sin\phi_i, \phi_i)$ back along the

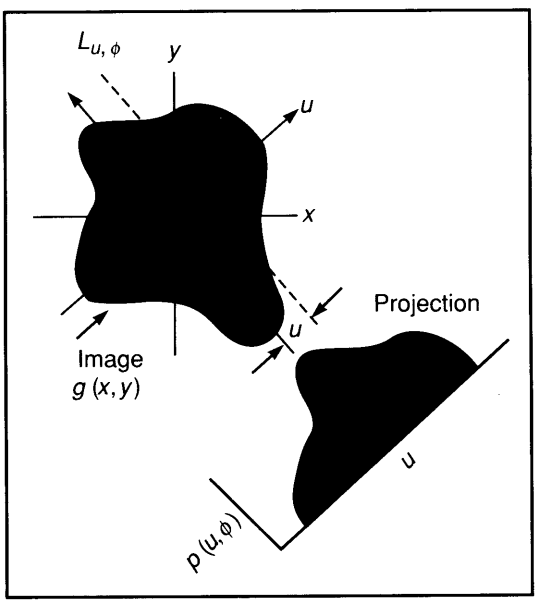

Fig. 5—Notation for transmission tomography.

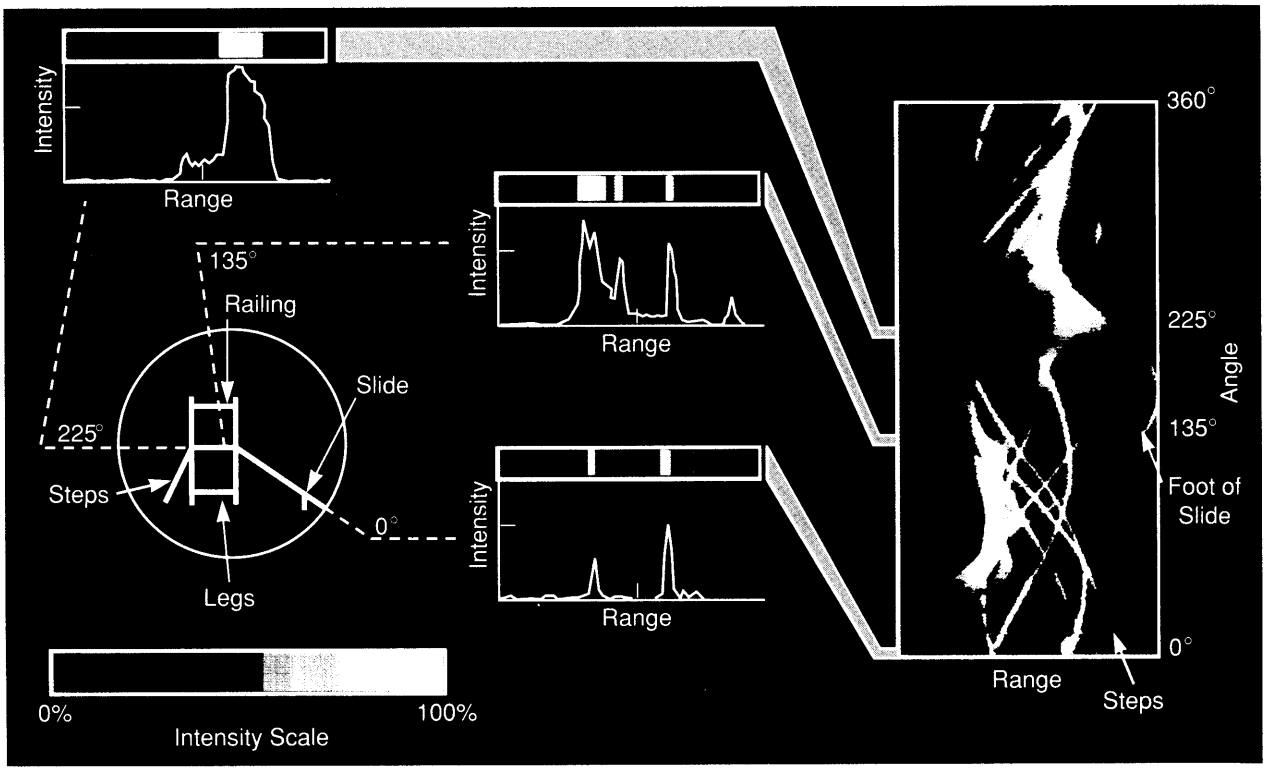

Fig. 6—Projections of a playground slide at many angles for a range-resolving radar form the input to the tomographic reconstruction. The signal versus range for three selected angles appears in two forms: a line plot and a color-coded bar. The bars can be compressed and combined into a color plot of range versus angle, shown at the right.

viewing direction, and then summing over all projection angles ϕ_i. This elementary method generally produces a starlike pattern of streak artifacts, which results in a low-quality image. To provide a better reconstruction, each projection can be modified before back-projection by a filtering operation in which the magnitude of each Fourier component of each projection is increased in proportion to the magnitude of its spatial frequency $|k|$. The image $g_{FB}(x, y)$, reconstructed by using filtered back-projection, is given by

$$g_{FB}(x, y) = \sum_{i=1}^{m} q(x \cos \phi_i + y \sin \phi_i, \phi_i)$$

where the modified projections $q(u, \phi)$ are given by

$$q(u, \phi) = \mathcal{F}_k^{-1}\{|k| \mathcal{F}_u[p(u, \phi)]\}.$$

$\mathcal{F}_u$ denotes the Fourier transform with respect to u, while $\mathcal{F}_k^{-1}$ denotes the inverse Fourier transform with respect to k. The angle of the ith projection is ϕ_i, and m is the number of projections.

In the application of tomography to laser radar data, the reflective projections (range, Doppler, or angle-angle) serve as input for the respective reconstruction algorithms. In the case of range or Doppler measurements, the projections $p(u, \phi_i)$, $i = 1, \ldots, m$ are processed as discussed above. The angle-angle measurements are processed with a modified version of back-projection described in a later section. For all three measurements, it is assumed that the viewing directions and a common point of reference for the projections are known or can be estimated.

For the range or Doppler measurements described, the large amount of input data is conveniently displayed, as shown in Fig. 6. This figure depicts a set of projections measured in 1°

increments around 360° for a range-resolving radar. The data are displayed by color-encoding intensity versus range for the 360 angles, as shown at the right of Fig. 6. From the display one can follow discrete reflectors as their projected range varies sinusoidally with angle. The amplitude of the sine wave is the distance of the reflector from the axis of rotation, while the phase represents the polar angle at the origin of the reflector with respect to a common point of reference. The next three sections present laboratory and field measurements taken over a range of viewing directions with three laser radars.

Reflective Tomography from Range-Resolved Measurements

This section describes range-resolved measurements, using a visible, short-pulse laser, of test objects on an indoor ground range. Two receivers are utilized: a photomultiplier tube connected to a transient digitizer, and a streak camera connected to a vidicon. The former has better sensitivity, while the latter has better range resolution. More details on the experimental setup and the results are described in Refs. 3 and 4.

Each receiver views objects up to 2 m in length on a 10-m indoor range, as shown in Fig. 7. The illumination comes from a frequency-doubled, Quantel Nd:YAG, pulsed laser that produces 532-nm pulses of 26 mJ with pulse lengths ≈100 ps FWHM. The laser pulses are diverged by a ground glass to produce uniform illumination and millimeter-sized speckles on the object. Objects are mounted on a single-axis rotator with a vertical axis of rotation and oriented so that the projections lie in the desired plane. Two calibration plates are used

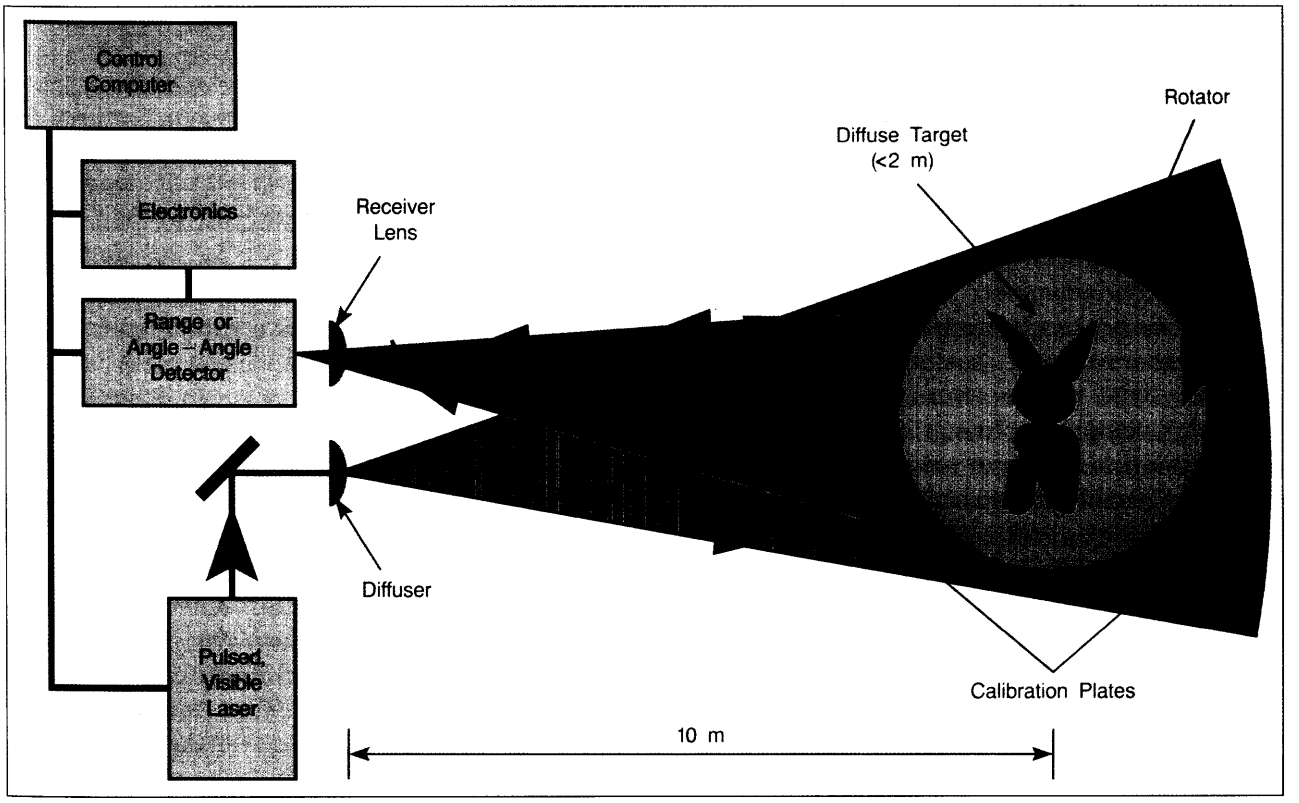

Fig. 7—The laboratory setup for range-resolved and angle-angle-resolved measurements. The pulsed laser illuminates the object on the rotator. The reflected light is received by one of two time-resolving (range-resolving) detectors, or an angle-angle detector, and then processed.

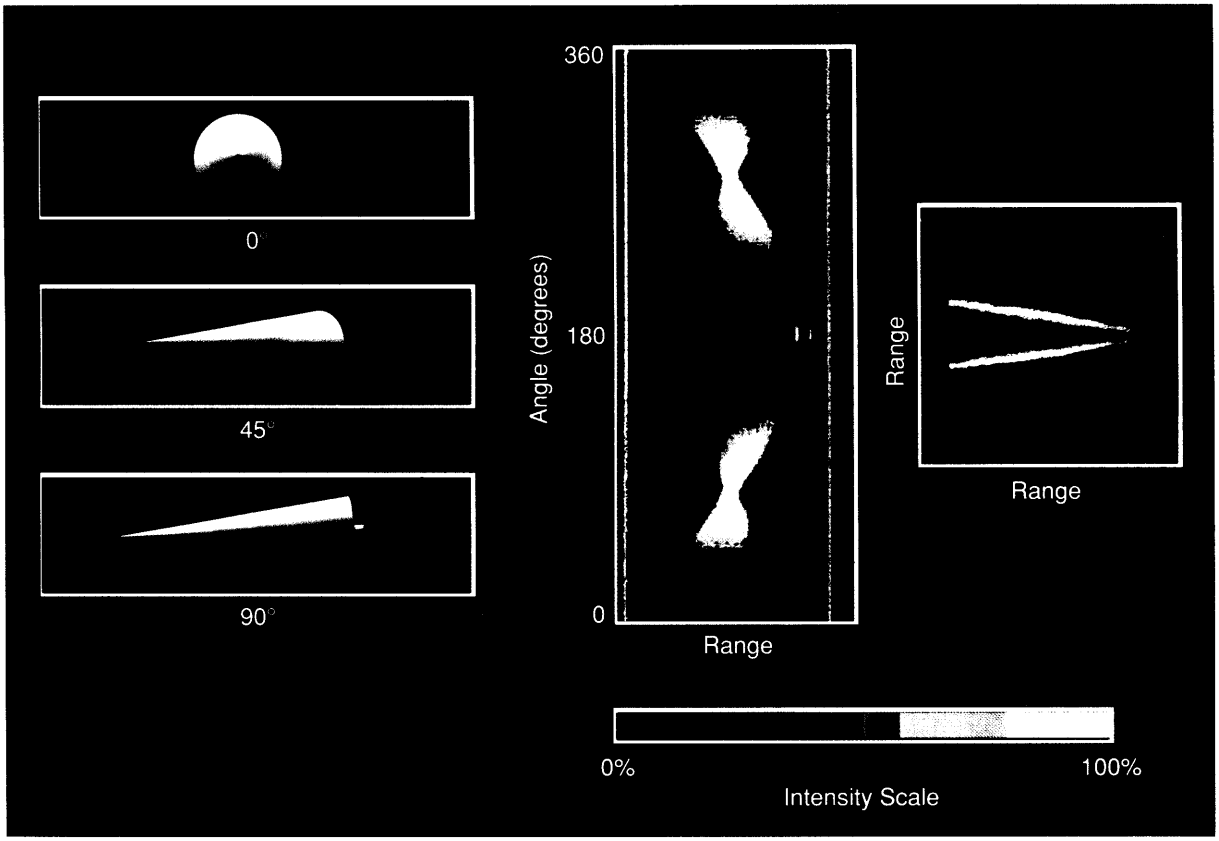

Fig. 8—Photographs (left), range-resolved data (center), and reconstruction (right) of an aluminum cone. The range-resolved data have a range extent of 2.5 m along the abscissa and angles from 0° at the bottom to 360° at the top along the ordinate. Intensity is coded in color. The vertical bars at the edges of the range-resolved data are the returns from the stationary calibration plates.

as stationary range markers and intensity calibrators.

Each of the two receivers records the time variation of optical input signals. The important characteristics are time resolution, time window, and sensitivity. In the first receiver, the reflected light is detected by a Hamamatsu R2083 photomultiplier tube and recorded every 100 ps with a Tektronix 7250 transient digitizer. The detector is photon-noise-limited and has a time resolution of 750 ps in a window of 400 ns, which yields a range resolution of 12 cm in a range window of 64 m. In the second receiver, the reflected light is detected by an E.G. & G. Energy Measurements streak camera, attached to an ITT 40-mm image intensifier and an RCA4804 vidicon. An 8-bit A/D converter digitizes the output. This receiver is not photon-noise-limited but has a time resolution of 250 ps in a window of 25 ns, which yields a range resolution of 4 cm in a range window of 4 m.

In a typical experiment, the object is viewed at many directions around the rotator's vertical axis. At each direction the receiver is triggered once, and a computer stores the data. After object data at all the desired viewing directions are acquired, the entire data set is processed.

For a first example, an object with a simple shape was imaged. The left and center panels of Fig. 8 show photographs and the data for an aluminum cone of 170-cm length and 53-cm diameter. The right panel of Fig. 8 demonstrates the feasibility of reconstructing an image of the cone with reflected light. The reconstructed image is the outline of the cone as viewed from

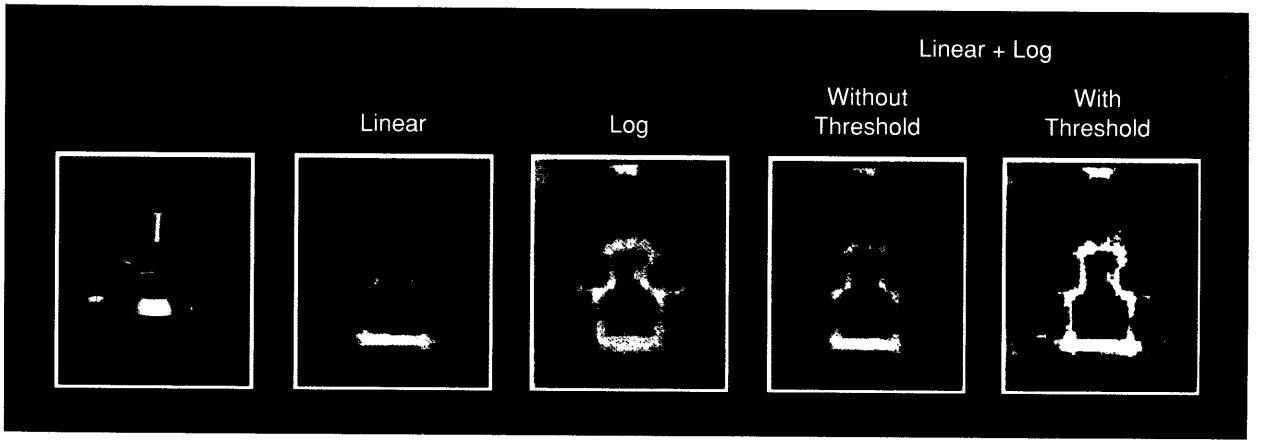

Fig. 9—Photograph and reconstructions of a model of a DSP satellite.

above, along the axis perpendicular to the plane of rotation. The image is an accurate representation in scale and geometry of the object when viewed in green laser light.

For a second example, Fig. 9 shows laboratory images of an object with a more complex structure: a model of a DSP satellite (an early-warning satellite launched in 1971). The model, constructed of styrofoam and wood and painted silver with aluminum solar panels, was positioned with the parabolic antennas and the body axis in the horizontal plane, so that the projection image shows the same view as the photograph. The green light reflected from the model has a wide dynamic range because of the bright specular solar panels and the dim diffuse wood body. The effects of enhancing portions of the dynamic range by data scaling are shown in the four reconstructions. From left to right, the data scalings are (1) linear scaling, (2) logarithmic scaling, (3) linear added to logarithmic without thresholding, and (4) linear added to logarithmic with thresholding. Linear scaling without thresholding makes the specular reflections dominate. The fainter diffuse reflections appear brighter with the logarithmic scaling. The sums (3) and (4) show the detail contained in the images and indicate that an outline could be extracted, perhaps for input to an object recognition algorithm.

Finally, we imaged a specular object with many contours: a five-foot toy rabbit. The material is smooth plastic with a variety of colors. The rabbit is mounted face up in the horizontal plane to provide the best cross section to image. Figure 10 shows the rabbit, the range-resolved data, and the reconstruction, which has high contrast and is easily recognizable by the eye.

Reflective Tomography from Doppler-Resolved Measurements

This section demonstrates the use of 1-D Doppler-resolved projections to form a 2-D tomographic image of a rotating object. The Firepond 10.6-μm CO_2 narrowband laser radar [14] and the 5.4-km ground range were used to make Doppler-resolved measurements over time (Doppler-time-intensity, or DTI) of a scale model of a Thor-Delta rocket body [5]. Figure 11 shows a diagram of the experimental setup. The model was rotated at approximately 1 rpm around an axis perpendicular to the sensor LOS. The return energy was detected by a heterodyne receiver and digitized at 256 kilosamples/s. Data were recorded over 360° in 1° angular increments and averaged over 5° to reduce speckle. Tomographic reconstruction using these data produces a 2-D image of the model as projected onto a plane perpendicular to the axis of rotation.

Figure 12(a) shows a photograph of the aluminum model of the Thor-Delta rocket body. The model was rotated around an axis perpendicu-

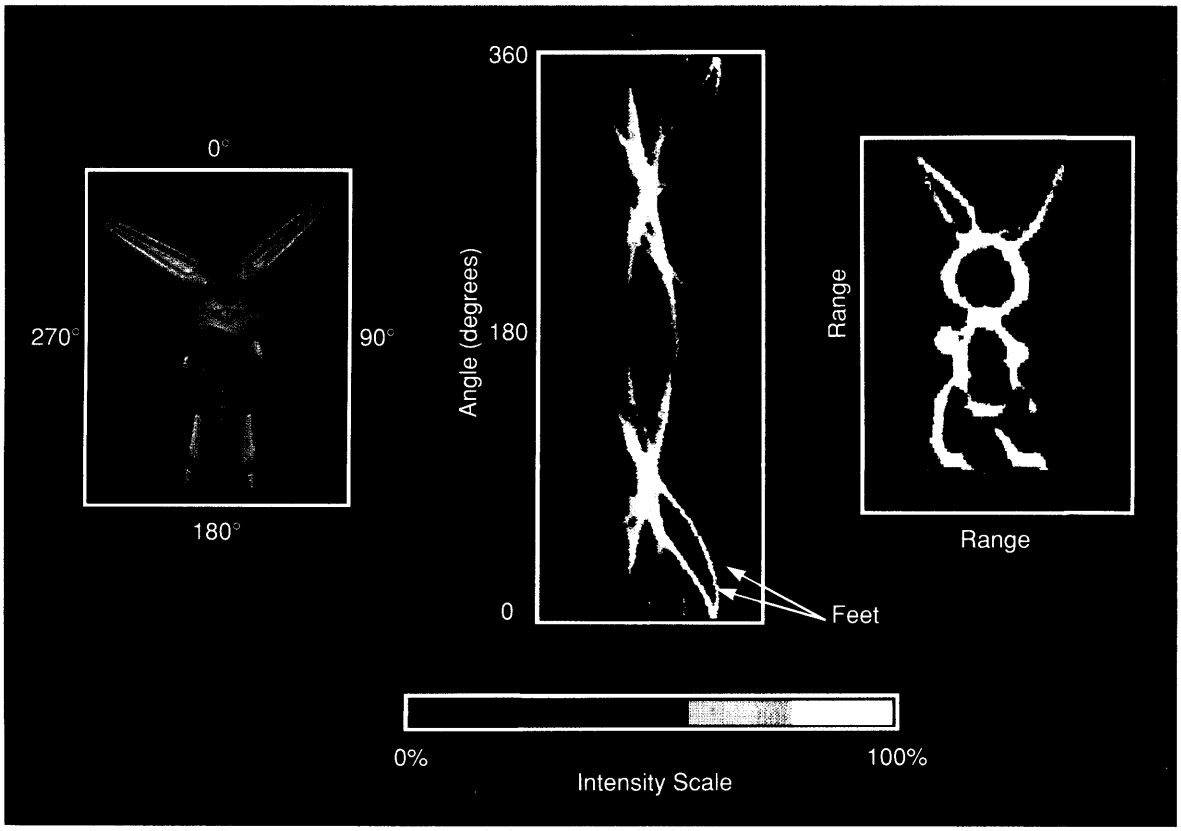

Fig. 10—Photograph (left), range-resolved data (center), and reconstruction (right) of a child's toy rabbit. The range-resolved data have a range extent of about 1 m along the abscissa and angles from 0° to 360° along the ordinate.

lar to the axis that passed through the center of the model body; this object motion is analogous to end-over-end tumbling. Figure 12(b) shows the DTI data of the object. Notice that the Doppler signature of the object is added to the zero-Doppler clutter (center stripe), and that the signature is complicated. In addition, the aluminum is specular near normal incidence, which causes bright reflections when sections of the model are normal to the sensor LOS. In general, individual specular reflections do not persist as the object rotates. Figure 12(c) shows how the filtered back-projection technique leads to the reconstruction of the Doppler image of the Thor-Delta model. With the optimal geometry chosen for these measurements, the image appears as a projection onto a plane that is perpendicular to the axis of rotation. Preprocessing the data before image reconstruction can enhance the desired features.

Unlike a reconstruction from range-resolved projections, a Doppler-resolved reconstruction is not a simple outline of the object. This result is due to the reflective properties of typical materials as well as to the geometry of range-resolved versus Doppler-resolved measurements. Materials typically have high reflectance at normal incidence and low reflectance at grazing incidence. This variation in reflectance results in bright edges in the reconstruction with range-resolved measurements, since an edge of the object is reconstructed from the projections that view the edge at normal incidence. On the other hand, with Doppler-resolved measurements an edge of the object is reconstructed from the projections that view the edge at grazing incidence, which results in low-intensity edges in the reconstruction.

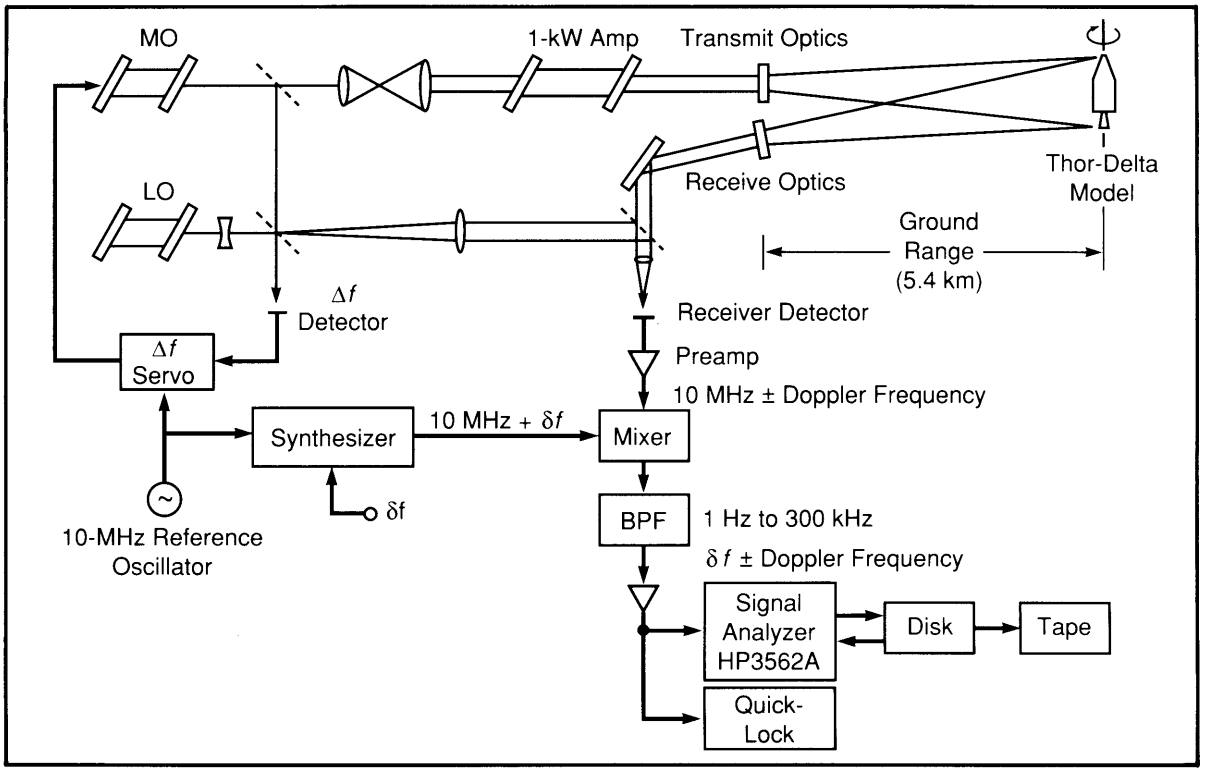

Fig. 11—Experimental setup of the 5.4-km narrowband ground range at Firepond. This system measured the Doppler-time-intensity projections of the aluminum Thor-Delta rocket model.

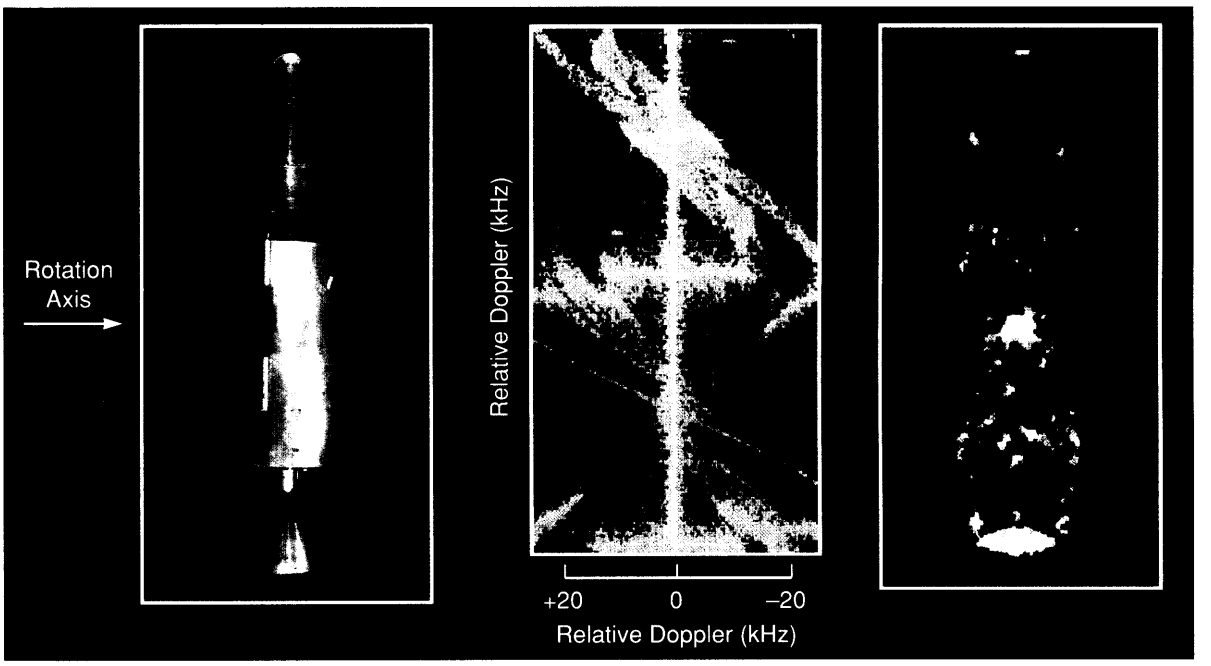

Fig. 12—A photograph (left) of an aluminum Thor-Delta rocket model. The axis of rotation passes through the center of the model and is perpendicular to the model's cylindrical axis. The 10.6-μm Doppler-resolved data (center) of the Thor-Delta rocket model. The zero-Doppler clutter reconstructs as a bright spot in the center of the image. A reconstructed image (right) of the Thor-Delta model.

Reflective Tomography from Angle-Angle Measurements

The previous two sections describe combining 1-D data to form 2-D projection images; this section describes combining 2-D data to form 3-D projection images. The 3-D projection image—the tomographic reconstruction of the 2-D images—approximates the size and shape of the object. We describe the laboratory setup, the results for one object, and some trade-offs concerning the parameters of the experiment.

The laboratory data come from a digital angle-angle camera that records reflected light from an object. The object is mounted on a turntable, so that many views can be imaged. The beam of a doubled, pulsed, Nd:YAG laser is diffused to illuminate objects of 30-cm-to-200-cm length on an indoor range of 10 m. The objects reflect the green laser light (532 nm) diffusely, so that light is collected over wide angles. Unless the test object is polished to optical quality, diffuse reflections (typical for visible wavelengths) yield sufficient signal at many viewing directions. At each viewing direction, the reflected light is imaged onto a TV camera, digitized, and stored for later reconstruction. Typically we take 5° steps around a great circle and use at least 100 × 100 pixels, which provides data that are more than ade-

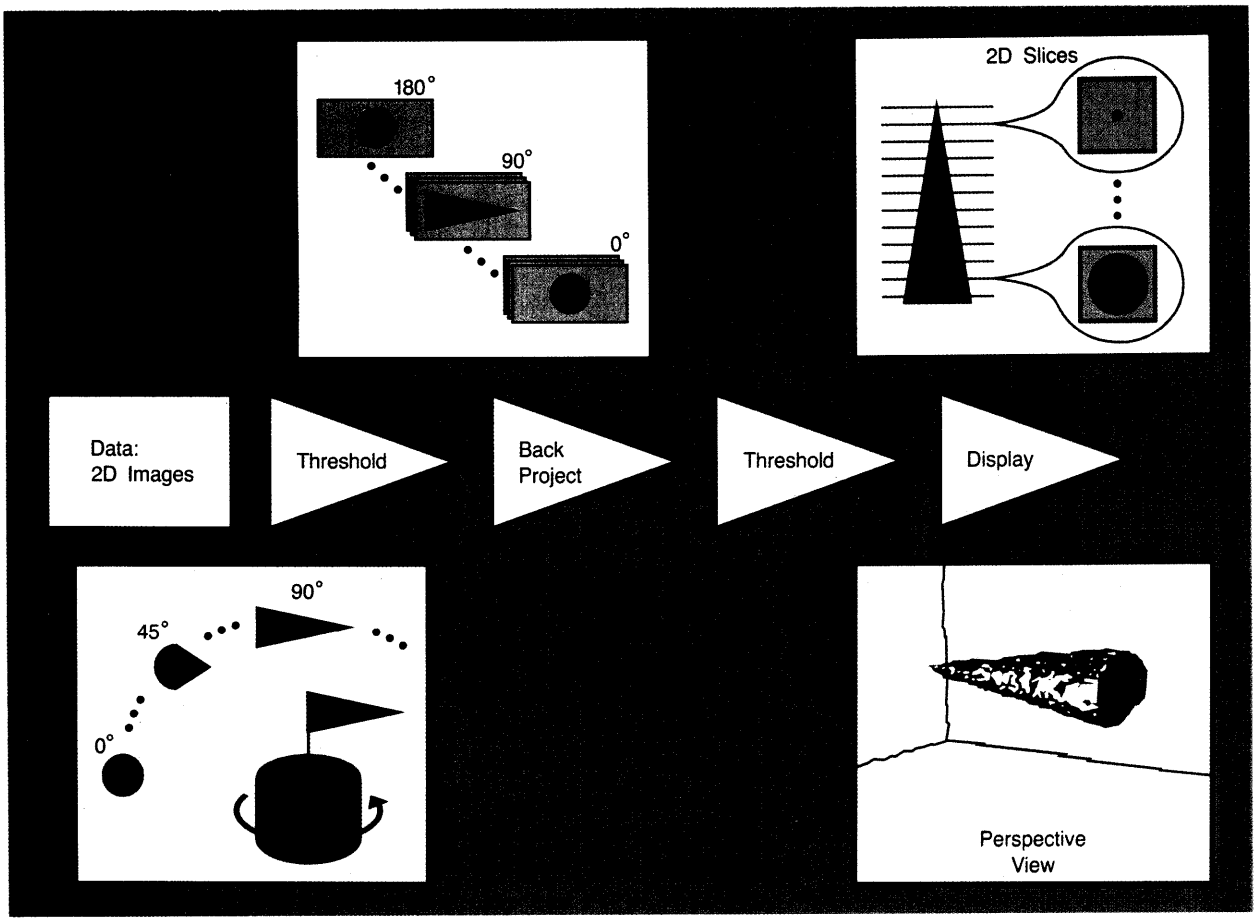

Fig. 13—The creation of a 3-D image with 2-D angle-angle images and tomography. In this method, a threshold, a back-projection, and a second threshold are applied to the input 2-D data to form the 3-D reconstruction. The reconstruction can be displayed as 2-D slices (as in a CAT scan) or as a perspective view.

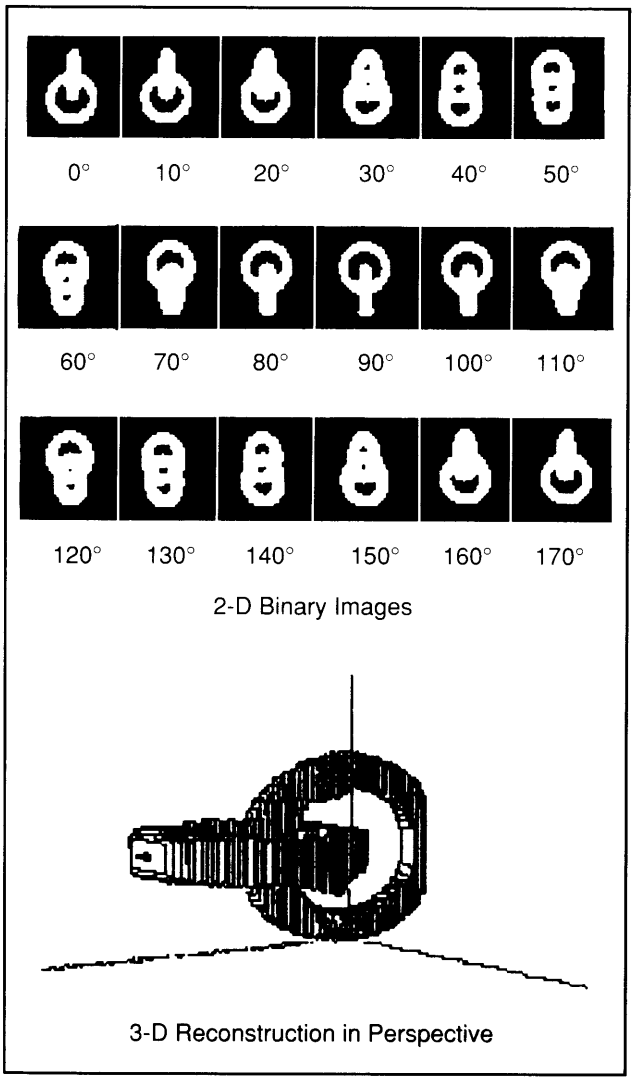

Fig. 14— Laboratory 2-D images and tomography create a 3-D image of two interlocking toroids. The input data were taken in 5° steps around a great circle, although only one-quarter of the input 2-D images are shown. The 3-D reconstruction is drawn in perspective and is a solid model of the toroids.

quate to produce the 3-D image. Figure 7 illustrates the laboratory setup.

Figure 13 shows the process of reconstruction. Variation in intensity is eliminated in each 2-D image by selecting a threshold level to produce a black-on-white silhouette: each image pixel is called black (or 1 in the computer) and each background pixel is called white (or 0 in the computer). The thresholding is used to limit the dynamic range on the 3-D reconstruction. Sufficient signal to noise of the 2-D images is required, so that the process of thresholding produces accurate silhouettes. The tomographic reconstruction uses back-projection to build an image in a reconstruction volume. The image built up by summing the projections from all aspect angles is a solid model of the object.

As displayed, the process is really two steps: the first step reconstructs slices of the object, and the second step combines slices into a 3-D silhouette. This process is similar to medical CAT scans. To extract 3-D information, a second threshold is selected and applied to the set of slices. Generally, the level of the second threshold is equal to the number of views; in other words, the image is the set of points that have contributions from all the views. The final result can be displayed as a set of slices or as a perspective view of the 3-D model. These results can be generalized to views from arbitrary directions.

Figure 14 illustrates the process of image reconstruction for two interlocking toroids (actually two worn auto tires) mounted at the center of our turntable and rotated through 360° in 5° steps. The black tires reflect enough light to produce clean binary images. The reconstruction, which is formed by using a threshold equal to the number of views, yields a recognizable solid model.

The reconstruction above uses a large number of views (72), high angular resolution ($\approx 100 \times 100$ pixels), high signal to noise (pulsed laser with a low-light-level TV detector), and a diffuse test object. All of these conditions can be relaxed, depending on the ultimate use of the data. For a high-fidelity 3-D image, a high density of views is needed. For quantitative shape information, mass moments of the image can be calculated to compare the image to a model or another object whose moments are known [15]. For crude orientation estimates, using mass moments of a tall cone, our work indicates that only a few views are needed (a minimum of three equally spaced around a great circle), provided enough angular pixels are available (a minimum of 30 along the cone axis). The pulsed laser gives high signal to noise, but

similar 2-D images can be obtained from bright ambient light. Lower signal to noise introduces a higher probability of false pixels in the 2-D binary images (which leads to holes in the image, or spurious background); one compensation is lowering the second threshold. A scanning laser radar can be employed as long as the 2-D images are registered in angle. Finally, we have restricted our views to a great circle, but arbitrary viewing directions from anywhere on the sphere are possible.

Discussion

This paper describes the use of tomographic techniques to process three types of laser radar data. For each type, the data are taken from many viewing directions to form a set of projections of the object. When processed, they produce a visual image (with an additional dimension) that can be used to estimate the object's structure. Each example of range-resolved data shows a 2-D image that accurately represents the size and projected shape of the test object, whereas, in the input data, size and shape are not readily apparent. The example of Doppler-resolved data shows a 2-D image that constitutes true narrowband imaging. The example of angle-angle-resolved data shows a 3-D image that reveals the size and shape of the object and provides an estimate of its 3-D structure. In each of the three examples, the image reconstruction presents a more complete picture of the object: each reconstruction reveals characteristics not apparent in the input data. All three examples are, however, ideal situations because they describe laboratory setups with high resolution, high signal to noise, and a large number of views. This section discusses several questions motivated by the initial experiments.

How do resolution, number of views, and registration affect the data? For both 2-D and 3-D tomographic imaging (and higher dimensions), the resulting image resolution is governed by the resolution and quality of the individual laser radar measurements, the density (or number) of individual views, and the accuracy with which the individual measurements can be registered or related to a common point. These issues must be addressed in detail before the reconstruction techniques can be applied to a specific problem, for example, the orientation of a tall cone of the previous section. To minimize the data collected (to reduce acquisition time or to save storage space) few views at low resolution are needed. Registration is necessary only to the width of a resolution cell, not a wavelength as in coherent addition of data.

How do complex motions degrade the results? In laboratory measurements, both a common origin and the viewing directions for all the projections are known. In a practical scenario, the objects of interest may execute complex motions with unknown rotation rates. In general, to apply these tomographic techniques the relative dynamics between the object and sensors must be known. In some cases, the dynamics may be derived from the measurements themselves. In the case when multiple range-resolving sensors take data simultaneously, no knowledge of dynamics is required. Furthermore, the independent measurements need to be aligned only to a range-resolution cell and not to a wavelength. This alignment puts fewer requirements on the single-sensor and the multiple-sensor scenarios, and with proper multiple-sensor geometry allows imaging of both rotating and nonrotating objects.

How do the results reported here compare to the results from microwave radar? The problem of reconstructing images from reflective microwave radar data by using tomographic techniques has been addressed by many researchers in the radar community [6–9]. In general, the diffuse scattering characteristics of a material increase with decreasing wavelength. Our results indicate that better image definition and improved resolution come from surfaces with a significant diffuse reflectance component. Improved images can thus be expected at laser wavelengths.

Can tomography be applied to range-Doppler measurements? Two-dimensional images can be obtained directly with laser radars that resolve the object in range-Doppler dimensions. As with 2-D angle-angle images, applying to-

mographic techniques to 2-D range-Doppler data to obtain 3-D reconstructions may be possible. In addition, an interesting application of tomographic imaging exists in the range-Doppler domain. It is possible to sample a single 1-D projection of the 2-D range-Doppler image with a single linear FM-chirp waveform for an object that has both range and Doppler extent [16, 17]. Projections at different angles can be obtained by changing the slope of the transmitted linear FM chirp. Since these data are projections in the range-Doppler space, 2-D range-Doppler images can be generated by applying tomography. Images formed in this way overcome some of the limitations of traditional range-Doppler imaging that uses repetitive waveforms.

What are some potential applications of these image-reconstruction techniques? New developments for remote sensing and imaging have applications in surveillance, medicine, machine vision, toxic environments, manufacturing quality control, and fusion plasma diagnostics.

For example, in robotics a detailed image of an object may be needed to grasp the object. By using the surface in the image, tangent lines could be drawn analytically to define grasping points.

As a second example, for transient events many sensors can be positioned at important aspect angles and triggered simultaneously to provide instantaneous input to the reconstruction algorithm [18]. The result is a snapshot in time to record the event for subsequent study.

As a third example, space surveillance could be performed by using laser radars from ground-based or airborne platforms. A single sensor on the ground could view spin-stabilized satellites or tumbling bodies in low earth orbit, in a wide range of directions. Other satellites, such as gravity-gradient-stabilized satellites that always point down, or geosynchronous satellites that remain fixed over one location on the equator, would offer fewer viewing directions for a single ground-based or space-based sensor. In such cases an array of ground-based receivers or active sensors could be used to extend the range of viewing aspects. The technologies required for using tomographic imaging techniques with laser radars are currently available.

Summary

We have applied tomographic image-reconstruction techniques to three types of laser radar reflective projections: range, Doppler, and angle-angle. Each reconstruction is an image of the object illuminated by the laser radar: a 2-D image formed from 1-D data or a 3-D image formed from 2-D data. As in all tomography, the input data must be taken from many viewing directions. The images are formed from laboratory measurements by using standard tomographic techniques. The reconstructions reveal detailed characteristics of the objects, and indicate that high-resolution images can be formed by using current laser radars.

Acknowledgments

Many individuals contributed to efforts on tomography in the Laser Radar Measurements Group. On the basis of a suggestion from W.E. Keicher, R.E. Knowlden originally considered in detail the use of tomography for combining Doppler measurements. D.R. Cohn assembled material on tomography in medicine and plasma research and presented a group seminar. W.E. Keicher suggested a novel reconstruction technique. E.F. Breau, and J.R. Senning helped study and implement a number of algorithms to combine existing Doppler-resolved measurements and computer-generated range-resolved data. L.J. Sullivan, D.G. Kocher, R.N. Capes, L.W. Swezey, J.A. Daley, R.A. Westberg, J.M. Anderson, E.J. Christiansen, G.L. Peck, A.S. Ruscitti, and H.A. Weigel helped make the infrared Doppler measurements on different objects. D.I. Klick, B.K. Tussey, A.S. Lele, A.M. Beckman, J.R. Theriault, Jr., K. Whittingham, and E.F. Breau helped obtain and process visible range-resolved measurements of a cone. D.I. Klick, D.P. Ryan-Howard, B.K. Tussey, J.R. Theriault, Jr., and A.M. Beckman helped make visible range-resolved and angle-angle-resolved measurements on many objects. A.S. Lele

worked on angle-angle-resolved measurements. K.I. Schultz and M.F. Reiley helped compare laser radar tomography and microwave radar tomography. We thank Kenny Tussey for the loan of the toy rabbit.